Spectral Dips in Ion Emission Emerging from Ultrashort Laser-Driven Plasmas

S. Ter-Avetisyan,[1,2] M. Schnürer,[1] S. Busch,[1] E. Risse,[1] P.V. Nickles,[1] and W. Sandner[1]
[1]*Max-Born-Institut, Max-Born-Strasse 2a, D-12489 Berlin, Germany*
[2]*Institute for Physical Research, Ashtarak-2, 378410, Armenia*
(Received 22 September 2003; published 8 October 2004)

Deep dips in MeV ion spectra are obtained from water droplet targets irradiated by intense [$(0.5–1.2) \times 10^{19}$ W/cm^2] and ultrashort (35 fs) laser pulses. The existence of these dips is ascribed to the generation of a multielectron-temperature plasma, which is confirmed by our experiments. An existing fluid model based on hot-electron components with significantly different temperatures is consistent with the behavior we observe in the ion spectra of the femtosecond laser-driven interaction. The model provides a good simulation of the observed spectral dips and allows us to establish important parameters such as hot- and cold-electron temperatures and the respective electron density ratios. The result may be of interest for spectral tailoring of proton spectra in future applications of laser-generated proton beams.

DOI: 10.1103/PhysRevLett.93.155006 PACS numbers: 52.50.Jm, 41.75.Jv, 52.38.Kd

In recent ultraintense ($I\lambda^2 > 10^{19}$ W cm^{-2} μm^2) laser-plasma interaction experiments, many interesting phenomena have been demonstrated [1]. Several physical mechanisms have been considered for the appearance of high-energy electrons and have been proposed as a way to understand the generation of ions with kinetic energies of several tens of MeV during the short laser-pulse interaction with dense plasmas [2–6]. A strong correlation was found [7] between the highest proton energies and the hot component of a plasma-electron distribution. A theory has been developed [8,9] for the free expansion of the laser plasma with hot (T_h) and cold (T_c) electron temperature components as a way to treat these nonequilibrium effects and to describe the ion energy distribution. It was shown that the energy fraction carried by fast ions depends on the temperature and concentration of the electrons in the plasma. This leads to an ion-emission velocity spectrum whose most notable feature is a pronounced dip in the distribution [10]. The slopes of the upper $[-(M/ZkT_c)^{1/2}]$ and lower $[-(M/ZkT_h)^{1/2}]$ asymptotes in the ion velocity spectrum make possible a determination of the effective absolute hot- and cold-electron temperatures [11]. (Here, M is ion mass, Z is charge state, and kT is cold- or hot-electron energy.)

The dip in the velocity distribution corresponds to an internal electrostatic sheath appearing due to hot- and cold-electron isothermal expansion, where ions are strongly accelerated in a small region. This dip develops in a region of self-similar flow where the ions experience rapid acceleration due to an abrupt increase in the electric fiend. This increase occurs at the location in the expanding plasma where most of the cold electrons are reflected, corresponding to a step in the ion charge density. (See Fig. 6 in [11].) The depth of the dip as a function of the peak field is a sensitive function of the hot- to cold-electron temperature ratio T_h/T_c in the ion spectra, while the position in the spectrum depends on the hot- to cold-electron density ratio n_h/n_c.

In a very short pulse (35 fs) and high intensity laser plasma, several groups of electrons with different temperatures can be generated [12], which could then cause multiple dips in the ion energy spectra. No hint of this has been observed so far, and therefore detailed measurements of the ion and electron spectra are required to find correlations between these processes. Quite recently, Allen *et al.* [13] found weak modulations in the high-energy tail of MeV proton spectra, which have been ascribed to the influence of different ion species in the accelerated beam.

In this Letter, we report precise measurements of the spectral density distribution of the ion emission from plasmas created by 35 fs laser pulses at intensities of $(0.8–1.2) \times 10^{19}$ W/cm^2. The diagnostics allowed for single-shot registration of each pulse. A pulse from a Ti:Sapphire laser [14] with a maximum energy of 750 mJ, a diameter of 70 mm, and a repetition rate of 10 Hz was focused with an $f/2.5$ off-axis parabolic mirror onto water droplets of $\sim$20 μm diameter [15]. Incidentally, we also used heavy water droplets without, however, observing any appreciable isotope effect on the phenomena discussed in this Letter. Hence proton and deuteron spectra will be discussed interchangeably. This is, to our knowledge, the first observation of these dips in ultrashort (sub 50 fs) high intensity laser-plasma interaction experiments. Measurements were made of ion spatial and energy distributions, x-ray spectral emission properties, the electron spectrum emitted, and the correlation of maximum electron energies with the cutoff energies of proton and deuteron spectra.

The dip phenomenon observed is discussed on the basis of the generation of ion-accelerating electric fields,

caused by different energy components of the electrons. These define the acceleration potential for the ions at the high- and low-energy parts of the spectrum [10]. Because of a high ratio of the "hot"- to "cold"-electron temperatures (T_h/T_c), a dip in the ion energy spectrum will appear [11]. The hot electrons can be produced by (i) the ponderomotive potential of the laser [16,17], (ii) fast plasma waves [18], and (iii) the laser field itself [19]. These mechanisms are not mutually exclusive, and their relative contributions depend strongly upon the particular target and laser parameters.

Measurements of the ion energies have been carried out with a Thomson parabola spectrometer, into which the ions enter through a 200 μm aperture. The ions are detected by a 40 mm multichannel plate (MCP) coupled to a phosphor screen. The signal from the phosphor screen is imaged with a charge-coupled device (CCD) camera. An ^{241}Am α-particle source (energy 5.4 MeV) with known emittance is used to calibrate the setup [20]. This sensitive, calibrated detection technique allows the measurement of an ion spectrum from a single laser shot in absolute terms.

A typical camera picture taken with a single laser shot, showing ion traces from a heavy water droplet, is shown in Fig. 1. The deuteron spectrum deduced from this digital CCD image is shown in the inset. The intensity values are counted in energy bins according to the spectrometer dispersion. The most interesting features in the picture are the clearly visible dips along the deuteron trace. As mentioned before, the same feature has been observed for proton emission from water droplets and has been observed in backward (135° to the laser axis) as well as in forward (laser propagation direction) emission. The occurrence of the spectral dips was reproducible in the experiment, although the exact position, depth, and fine structure varied from shot to shot due to small variations in the laser parameters and beam alignment in our setup.

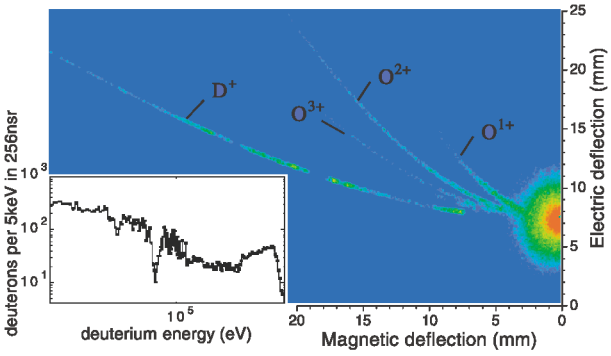

FIG. 1 (color). Color coded image from the MCP-phosphorous screen of an emitted ion spectra (deuterons, most intensive parabolic trace; others, oxygen; right blob, "zero" point: radiation impact along spectrometer axis) from a heavy water droplet taken from a single laser shot in backward (135° to laser propagation) direction with the Thomson spectrometer. In the inset, deuteron spectrum deduced from this digital CCD image. (Note that nsr is the collection angle of 10^{-9} sr.)

The generation of high-energy electrons is critical for ion acceleration scenarios, so we also measured the hot-electron spectrum. Electrons emitted in a direction transverse to the laser axis were deflected in a 0.27 T magnet and detected by GAFchromic film (HD-810). This film is sensitive to electrons above 10 keV due to its layer characteristic [20]. The measured time-integrated hot-electron spectrum (Fig. 2) shows a maximum at an energy of about 0.7 MeV with a tail expanding to 2 or 3 MeV.

From the measured electron spectra, we can deduce a hot-electron component with a temperature of (0.63 ± 0.03) MeV. This fits well with the energy the electrons can acquire from the ponderomotive force F_p of the laser pulse [21]: $F_p = -dU_p/dz$, $U_p(\mathrm{eV}) = 9.33 \times 10^{-14} I(\mathrm{W/cm^2})\lambda^2(\mu\mathrm{m})$, where U_p is the ponderomotive energy. This gives a potential energy of 0.6 MeV for our laser intensity, proving a rather efficient laser energy transfer to the electrons. Because up to 20% of the laser energy can be absorbed in energetic electrons [16], a significant number of electrons with energies of several hundreds of keV is produced, which can penetrate into the target. The electron impact ionization cross section is about 10^{-19} cm^{-2} at energies in the range of 400 to 500 keV [22], and so these highly energetic electrons can cross the target without being significantly slowed. As is visible in Fig. 2 (showing the hot-electron emission spectrum from a D_2O plasma), only highly energetic electrons can escape from the target because a space-charge field accumulates that captures hot electrons with energies below about 200 keV. Because of the target potential, the lower range of electron energies is trapped, and a virtual cathode is formed around the droplet. The potential due to these electrons and the estimated electron

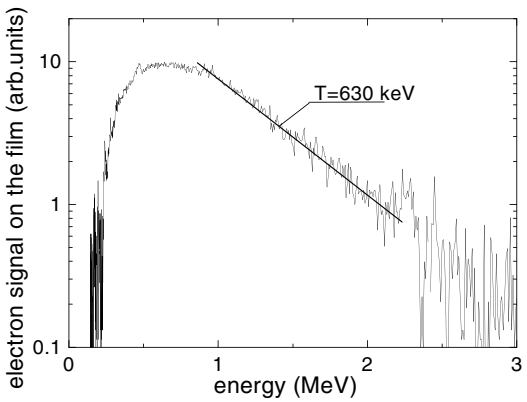

FIG. 2. Hot-electron energy distribution emitted from heavy water microdroplets at 35 fs, ~10^{19} W/cm^2 irradiation (superposition of ~50 000 shots on a GAF-HD-810 film electron spectrometer). Slope fits to an exponential decay with a temperature $T = 630$ keV parameter.

density is sufficient to create electrostatic acceleration fields of the order of 1 MV/μm [20], which, in turn, can accelerate ions to MeV energies. Electrostatic or magnetic fields around the target will influence the directionality of ion emission. For our spherical target, we expect a relatively isotropic ion-emission distribution, which can be shown by measurements [20,23].

Furthermore, a significant correlation between the maximum ejected electron energies and the deuteron cutoff energies could be directly established (Fig. 3) with the help of a redesigned Thomson spectrometer. In this setup, a second MCP was added to that side of the spectrometer where the electrons are deflected. This allowed us to measure in one laser shot the emitted ion and that part of the electron spectrum emerging at the same angle to the laser pulse. In Fig. 3, a variation in the maximum electron energy by only a factor of 1.2 changes the deuteron cutoff energy by a factor of about 5. This extreme sensitivity emphasizes the predominant role of the energy transfer to the electrons for the ion acceleration. Finally, these electrons leaving the target show that the space-charge field built up in the target is defined by target electron populations with a maximum energy of about 200 keV (the low-energy cut in the electron spectrum of Fig. 2). This space charge is responsible for the ion acceleration properties. Therefore, we studied the trapped hot electrons in further detail. According to a simple bremsstrahlung model [24], hard x-ray emission from the plasma is defined by the electron density distribution inside the target. For highly energetic electrons crossing the droplet, the target is "thin," so their bremsstrahlung is weaker and the spectral intensity is constant [25].

A calibrated x-ray CCD camera operating in a single-photon detection mode was used for energy-dispersive x-ray measurement [26]. In the experiments, the CCD camera was mounted at an angle of 90° to the laser propagation direction and at a distance of 100 cm from the plasma source. A 200 nm Zr filter and beam aperture was used to block the optical light and scattered x rays.

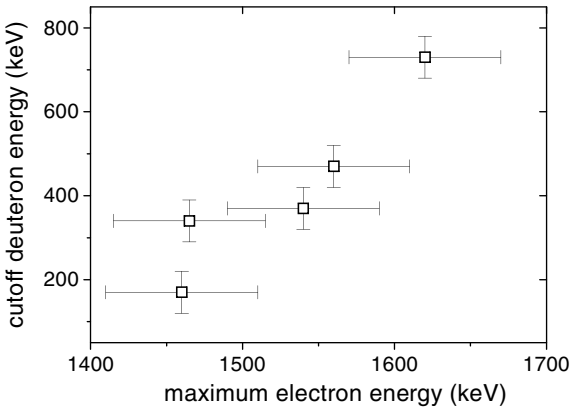

FIG. 3. Correlated maximum energies of emitted electrons and deuterons in a single laser shot.

The resolution of our spectral diagnostic is about 0.5 keV. A typical x-ray spectrum is shown in Fig. 4. The slope of the distribution shows the existence of multitemperature components and can be fitted assuming three different effective temperatures of about (7 ± 0.3) keV, (20 ± 4) keV, and (33 ± 12) keV.

Recently, a fluid model based on a *single electron temperature approximation* was applied successfully for high intensity laser-driven ion acceleration [27]. Accurate results could be obtained for the structure of the ion front, the ion energy spectrum, and the cutoff ion energy. In the present Letter, on the other hand, we explain the dips in the emitted ion spectrum (Fig. 1) by relying on the fact that we have an electron spectrum characterized by *several electron temperatures*. This is the precondition for application of the fluid model [8–10].

Figures 5(a) and 5(b) compare experimental proton and deuteron energy distributions from single laser shots with calculations based on the theory of Wickens *et al.* [8]. A reasonable fit for the depth and position of the dip in the proton spectrum [Fig. 5(a)] is obtained when the hot- to cold-electron temperature ratio T_h/T_c is assumed to be about 9.8, and the hot- to cold-electron density ratio n_h/n_c is about 1/100. Individual electron temperatures $T_c = 7.5$ keV and $T_h = 74$ keV compare quite well to the range of temperatures derived from the x-ray emission. Here, T_h is lower by a factor of about 2, but this can be due to the restricted linearity range (<50 keV) in the x-ray measurement. Also, if one takes into account that bulk ion energy scales with hot-electron temperature as $E_{\text{ion}} = 4.5\, T_h$ [9], a mean ion energy $E_{\text{ion}} = 330$ keV would be derived, in remarkably good agreement with the ion temperature inferred from the ion slope [Fig. 5(a)]. This is somewhat different from the original model where the ion energy is predicted to be similar to the hot- cf. cold-electron energies. A sharp proton cutoff energy occurs at

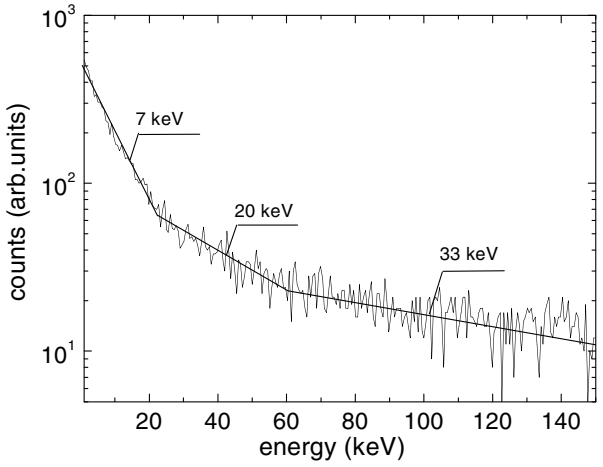

FIG. 4. X-ray emission spectra from a single droplet taken with an x-ray CCD camera operated in an energy-dispersive single-photon detection mode.

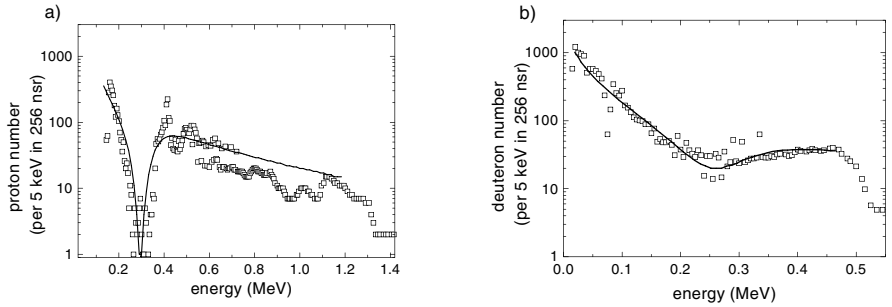

FIG. 5. (a) Single-shot proton and (b) deuteron spectrum with typical dips along the trace: squares, experiment; line, simulation (parameter cf. text).

about 1.3 MeV. Notice that the analytical velocity distribution derived in [8] breaks down if the temperature ratio T_h/T_c exceeds 9.9. In order to overcome this problem, a more complex electron velocity distribution was included in [10].

Another example of a deuteron energy distribution obtained from a heavy water droplet is presented in Fig. 5(b) where the cutoff energy occurs at about 0.55 MeV. Here the model with a hot- to cold-electron temperature ratio $T_h/T_c = 7.7$ and an electron density ratio $n_h/n_c = 1/25$ fits the measurement quite well. The individual temperatures are $T_c = 11$ keV and $T_h = 85$ keV. The model shows convincingly how small changes in T_e and n_e have large effects on spectral slopes.

In conclusion, we have measured, to our knowledge for the first time, significantly structured ion spectra from ion acceleration experiments when ultrashort (35 fs) laser pulses at intensities of about 10^{19} W/cm^2 interact with small spherical water droplet targets. The strong dependence of the emitted ion (cutoff) spectra on the electron energy distribution (maximum energy) could be demonstrated in single laser shots. Because of the short laser pulse, a hot-electron population is created that shows an apparent multitemperature behavior, as visible from x ray and maximum ejected electron energies. This, in turn, can cause strong dips in the ion spectrum, which was shown in previous fluid model calculations. Our results suggest that this model is also applicable for high intensity femtosecond laser-produced plasmas. Following this approach, such important parameters as hot- and cold-electron temperatures and the density ratio of hot- or cold-electron populations can be determined from ion spectra in ultrashort-pulse driven plasmas without the help of sophisticated 2D or 3D particle-in-cell simulations. It is worth noting that the results demonstrated here could open a way to tailor the ion spectra [28] from short-pulse laser-driven plasmas by choosing proper electron distributions appropriate to particular applications.

We thank D. Hilscher and U. Jahnke for stimulating discussions concerning the ion-emission feature, Howard R. Reiss for remarks and discussion, and H. Schönnagel and M. P. Kalachnikov for the laser system guidance. This work was partly supported by DFG-Project SFB-Transregio TR 18.

[1] D. Umstadter, J. Phys. D **36**, R151 (2003).
[2] G. Malka and J. L. Miquel, Phys. Rev. Lett. **77**, 75 (1996).
[3] E. L. Clark *et al.*, Phys. Rev. Lett. **85**, 1654 (2000).
[4] D.W. Forslund and J. U. Brackbill, Phys. Rev. Lett. **48**, 1614 (1982).
[5] A. P. Fews *et al.*, Phys. Rev. Lett. **73**, 1801 (1994).
[6] F. N. Beg *et al.*, Phys. Plasmas **4**, 447 (1997).
[7] S. J. Gitomer *et al.*, Phys. Fluids **29**, 2679 (1986).
[8] L. M. Wickens, J. E. Allen, and P. T. Rumsby, Phys. Rev. Lett. **41**, 243 (1978).
[9] L. M. Wickens and J. E. Allen, J. Plasma Phys. **22**, 167 (1979).
[10] Y. Kishimoto, K. Mima, T. Watanabe, and K. Nishikawa, Phys. Fluids **26**, 2308 (1983).
[11] L. M. Wickens and J. E. Allen, Phys. Fluids **24**, 1894 (1981).
[12] A. G. Zhidkov *et al.*, Phys. Plasmas **8**, 3718 (2001).
[13] M. Allen *et al.*, Phys. Plasmas **10**, 3283 (2003).
[14] M. P. Kalachnikov *et al.*, Laser Physics **12**, 368 (2002).
[15] O. Hemberg *et al.*, J. Appl. Phys. **88**, 5421 (2000).
[16] S. C. Wilks *et al.*, Phys. Rev. Lett. **69**, 1383 (1992).
[17] E. Lefebvre *et al.*, Phys. Rev. E **55**, 1011 (1997).
[18] T. Tajima and J. M. Dawson, Phys. Rev. Lett. **43**, 267 (1979).
[19] A. Pukhov *et al.*, Phys. Plasmas **6**, 2847 (1999).
[20] S. Busch *et al.*, Appl. Phys. Lett. **82**, 3354 (2003).
[21] W. L. Kruer and K. Estabrook, Phys. Fluids **24**, 430 (1985).
[22] http://physics.nist.gov/cgi-bin/Ionization/table.pl?ionization=H2O
[23] S. Karsch *et al.*, Phys. Rev. Lett. **91**, 015001 (2003).
[24] H. R. Griem, in *Plasma Spectroscopy* (McGraw-Hill, New York, 1964), p. 113.
[25] M. A. Blochin, in *Physik der Röntgenstrahlen* (Akademischer Verlag, Berlin, 1957), p. 70.
[26] S. Ter-Avetisyan *et al.*, J. Phys. D **36**, 2421 (2003).
[27] P. Mora, Phys. Rev. Lett. **90**, 185002 (2003).
[28] K. Nishihara *et al.*, Nucl. Instrum. Methods Phys. Res., Sect. A **464**, 98 (2001).